DOE/MC/25027--3112

DE92 012455

Ice Island Creation, Drift, Recurrences, Mechanical Properties, and Interactions With Arctic Offshore Oil Production Structures

Final Report

W.M. Sackinger
M.O. Jeffries
Fucheng Li
Mingchi Lu

March 1991

Work Performed Under Contract No.: DE-FG21-88MC25027

For
U.S. Department of Energy
Office of Fossil Energy
Morgantown Energy Technology Center
Morgantown, West Virginia

By
University of Alaska Fairbanks
Geophysical Institute
Fairbanks, Alaska

DOE/MC/25027-3112

Ice Island Creation, Drift, Recurrences, Mechanical Properties, and Interactions With Arctic Offshore Oil Production Structures

DOE

Please Recycle

DOE/MC/25027-3112
(DE92012455)
Distribution Category UC-124

Ice Island Creation, Drift, Recurrences, Mechanical Properties, and Interactions With Arctic Offshore Oil Production Structures

Final Report

W.M. Sackinger
M.O. Jeffries
Fucheng Li
Mingchi Lu

Work Performed Under Contract No.: DE-FG21-88MC25027

For
U.S. Department of Energy
Office of Fossil Energy
Morgantown Energy Technology Center
P.O. Box 880
Morgantown, West Virginia 26507-0880

By
University of Alaska Fairbanks
Geophysical Institute
Fairbanks, Alaska 99775-0800

March 1991

TABLE OF CONTENTS

EXECUTIVE SUMMARY

Research and engineering studies on first-year sea ice for over two decades has resulted in the design, construction, and operation of jacket platforms, of artificial islands, and of massive gravity structures which routinely withstand moving sea ice of thickness up to 2 meters. However, the less-common interactions between such structures and moving multiyear ice (≥ 3 meters thick), and also moving ice islands (10 to 60 meters thick) remain as the unknown and potentially most serious hazard for Arctic offshore structures. In this study, research was addressed across the complete span of remaining questions regarding such features. Ice island components, thickness distributions, scenarios and models for the interactions of massive ice features with offshore structures, all were considered.

Ice island morphology and calving studies were directed at the cluster of 19 ice islands produced in a calving from the Ward Hunt Ice Shelf on Ellesmere Island in 1983, and also at a calving from the Milne Ice Shelf in 1988. Offshore winds of 10 meters per second, with accompanying storm surge, were associated with the latter event, driven by a high-pressure condition over Greenland and a low-pressure cell over the Canadian Arctic Archipelago. The use of satellite imagery acquired by synthetic-aperture radar (SAR) was proven to be an effective tool in detecting such calving events.

The statistics of ice island dynamics, on both a short-term small-scale basis and also on a long-term basis, were studied. Typical wind velocities of 5 to 7.5 meters per second led to ice island speeds of about 0.014 of the wind speed, at an angle of 20° to the right of the wind direction.

Ice island samples were tested for their stress/strain characteristics. Compressive strength values ranged from 1.64 MPa at a strain rate of 2×10^{-7} s^{-1} to 6.75 MPa at a strain rate of 1×10^{-3} s^{-1}.

Scenarios for ice island/structure interactions were developed, and protective countermeasures such as spray ice and ice rubble barriers were suggested. Additional computer modeling of structure/ice interactions for massive ice features is recommended.

I. INTRODUCTION

Research and engineering progress on first-year sea ice, generally less than 2 m thick, has advanced considerably since studies on offshore oil-related problems were initiated 20 years ago. The results of the first-year ice studies cannot, however, be applied to multiyear ice (≥ 3 m thick) and ice islands (≥ 10 m thick). Unfortunately, there have been few studies of these larger ice masses, particularly in the context of interactions with offshore production structures. Consequently, there is a need for new data and observations of the large-scale physical and dynamic characteristics of multiyear ice and ice islands. The objective of this study was to provide the scientific knowledge and information required to predict forces on arctic offshore structures during interactions with massive multiyear sea ice floes and ice islands. Preliminary work on this topic has included identification of ice island components and thickness distributions, ice island drift trajectory variations, development and evaluation of scenarios and models for the interaction of massive ice features with offshore structures, and identification of possible measures to mitigate the hazard.

The term 'ice island' was coined over four decades ago to describe the tabular icebergs of the Arctic Ocean, particularly those which calve from the ice shelves located along the north coast of Ellesmere Island in the Canadian high Arctic (e.g. Koenig et al., 1952; Jeffries, 1987). Walker and Wadhams (1979) use the term 'thick sea ice floes' to describe undeformed congelation sea ice floes exceeding 6 m thickness, which have been reported occasionally in the Arctic Ocean. The multiyear landfast sea which grows alongside the ice shelves of northernmost Ellesmere Island is a well-documented source of thick sea ice floes; the detection of a thick sea ice floe calving at the Milne Ice Shelf in February 1988 is described in a later chapter of this report. There are undoubtedly other tabular iceberg and thick sea ice floe sources within the Arctic Basin, e.g. northernmost Greenland, Svalbard and the Soviet Arctic

Islands, but this report is concerned primarily with those originating from the Ellesmere ice shelves.

Although they are relatively few in number and areal extent in relation to the total amount of pack ice, the significance of the ice islands and thick sea ice floes is that they are the thickest drifting tabular ice masses in the Arctic Ocean. Consequently, the design and operation of arctic offshore structures must at least consider the possibility of interactions with ice islands and thick sea ice floes. For example, in May 1972, 433 ice island fragments ranging in size from <156 m to >300 m across were observed aground in the shallow waters of the southern Beaufort Sea from Mackenzie Bay, Canada to Point Barrow, Alaska (Spedding, 1977). Although this number of fragments represents an extreme example, probably related to the grounding and disintegration of a much larger ice island, it illustrates the possibility of ice island invasions of those potentially oil- and gas-rich offshore zones.

This report considers some aspects of the interaction of ice islands and thick sea ice floes with arctic offshore structures. Large-scale ice feature morphology and structure, ice island drift and dynamics, ice island/structure interaction scenarios, and some passive and active methods to mitigate that hazard are discussed.

II. ICE ISLAND MORPHOLOGY, STRUCTURE AND CALVING

There are at least nineteen ice islands shown in Figure 1, a visible band SPOT-1 satellite image taken over the Arctic Ocean near northern Ellef Ringnes Island on 28 July 1988 (see Figure 3 for location). The ice islands may be distinguished from the pack ice by a combination of features. A striped or ribbed texture arises from the linear surface undulations where meltwater accumulating in the troughs creates ribbon lakes with dark tones in summer. The ice islands have generally darker tones than the adjacent pack ice floes, again due to surface meltwater. The ice islands are often larger, with more distinct angular boundaries than the pack ice floes.

The largest ice island in Figure 1 is Hobson's Choice Ice Island, the largest presently known to exist in the Arctic. It calved from the Ward Hunt Ice Shelf in 1982-83 (Jeffries and Serson, 1983). All of the ice islands in the image probably originated from that same calving event, and they illustrate a number of morphological/structural features of interest in discussions of interactions with arctic offshore structures.

The ice islands' dimensions in Figure 1 range from a minimum of 0.2 x 0.3 km to a maximum of 5.7 x 8.7 km. Ratios of length to width (L-W) range from 1.25 to 4.0, and 79% of the ice islands have L-W ratios <3. Jeffries et al. (1988) found a comparable distribution of L-W ratios for a total of 53 ice islands observed and measured since 1946, including this group. It seems that L-W ratios less than three represent some highly probable ice island formation geometry, for reasons which are not yet clear.

The ribbed, dark-toned surface features of the ice islands correspond to that of the former shelf ice. In the case of Hobson's Choice, and probably for most of the ice islands in Figure 1, the shelf ice thickness at the time and location of the calving was about 42 meters. The ice thickness can be expected to decrease over time due to summer melting. The long-term rate of ice island thinning has not been studied systematically, but on a decadal time-scale it appears to average about 1 m per year for an ice island circulating in the Beaufort Gyre (Jeffries et al., 1988).

All of the ice islands have some sea ice attached to the shelf and in some cases they are completely embedded in multiyear floes (Figure 1). The sea ice is of two types; multiyear landfast sea ice (MLSI) and multiyear pack ice (MYPI), denoted 1 and 2 respectively in the SPOT image. The MLSI is particularly evident on the two largest ice islands; it was attached to the front of the Ward Hunt Ice Shelf at the time of calving and has remained attached to the shelf ice since then. Jeffries and Sackinger (1989) assume that the MLSI is about 20 years old, as much as 10 m thick, and comprises fresh, brackish, and sea ice layers, similar to the other extensive areas of MLSI on the north coast of Ellesmere Island.

The MYPI, is composed of consolidated ice rubble and floes welded together by refreezing meltwater. Measurements of the thickness of the MYPI attached to Hobson's Choice have not been made, but it is estimated to be 5-6 m thick (Jeffries and Sackinger, 1989). On Hobson's Choice the MYPI has accreted primarily in a triangular zone along the edge opposite the MLSI (Figures 1 and 2), with some accreted on the edge of the MLSI also. On the large ice island adjacent to Hobson's Choice, the MYPI has accreted against the MLSI, while numerous ice islands are completely engulfed by the MYPI (Figure 1). The SPOT image suggests that smaller ice islands (<2-3 km) tend to become embedded in MYPI, while on the large ice islands the MYPI tends to attach to the long edges, leaving the ends of the shelf ice exposed. Because of the greater water drag of the ice island, due to its deep keel, and also because of the large Coriolis force on the moving ice island resulting from its great mass per unit area, there is a differential velocity between pack ice and the ice islands. Tension events, new ice in adjacent leads, and frequent ridge-building along the ice island boundary, are probably responsible for the formation of the MYPI.

The addition of MYPI to ice islands is a means by which they can increase in area and mass. For example, Hobson's Choice Ice Island (Figures 1 and 2) originally had an area of 26 km^2 and a mass of 7.0×10^{11} kg (Jeffries et al., 1988), but with the

Figure. 1: Visible band SPOT-1 satellite image of Hobson's Choice and other ice islands surrounded by pack ice in the Arctic Ocean near northern Ellef Ringnes Island, N.W.T., 28 July 1988.

addition of the MYPI its area has increased to almost 34 km^2 and the mass to 7.4 x 10^{11} kg (Jeffries and Sackinger, 1989).

A two or three-component ice island has an unusual cross-sectional profile, with a non-uniform thickness (Figure 2). The MLSI and MYPI are considered to be integral parts of the ice island and they may remain attached to the shelf ice component. However, it is quite possible that the multiyear ice components may break off the shelf ice when it is drifting in open water in the southern Beaufort Sea (cf. Jeffries, et al., 1988, p. 83); hence, only shelf ice might remain and could directly contact a structure.

Much less is known about the morphology and structure of thick sea ice floes. Walker and Wadhams (1979) discuss their possible sources, occurrences, size, thickness and growth mechanisms. Those which break off the MLSI fringe of northernmost Ellesmere Island can be quite large.

For example, on 22 February 1988 the STAR-2 airborne synthetic aperture radar (SAR) was used to obtain 1:300,000 scale SAR imagery of the north coast of Ellesmere Island, N.W.T., Canada, for the Canadian Arctic Marine Ice Atlas. The SAR data was made available to us in April 1988 by the Canarctic Shipping Company Limited, Ottawa, Canada to assist with our surveys of the Ellesmere Island ice shelves. Analysis of the SAR imagery detected a massive ice calving from the Milne Ice Shelf (Jeffries and Sackinger, 1990).

The February 1988 SAR image of the outer part of the Milne Ice Shelf is shown in Figure 3a. The ice shelf is the second-largest remaining on the north coast of Ellesmere Island (Fig. 3b). The SAR returns from the ice shelf have an unusual ribbed texture of light and mid-grey returns related to the undulating surface topography of linear and curvi-linear hummocks and depressions. At the front of the Milne Ice Shelf is a roughly S-shaped, dark-toned (almost black) feature (Fig. 3a). This is interpreted as a recently refrozen lead and, it lies between the northwest front of the ice shelf and a detached piece of MLSI. This MLSI is the Milne

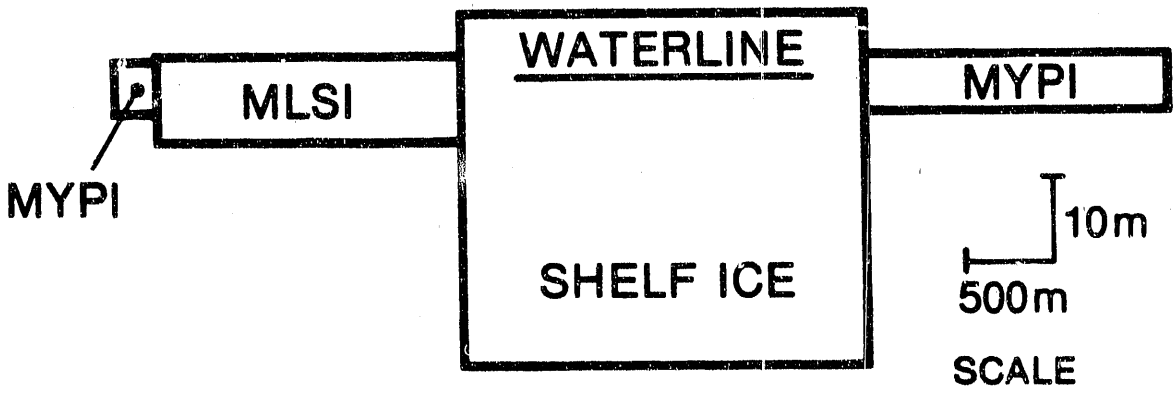

Figure. 2: Idealized cross-section profile of Hobson's Choice ice island showing the ice thickness variations due to the accretion of multiyear landfast sea ice (MLSI) and multiyear pack ice (MYPI) onto the shelf ice.

Re-entrant which, as the SAR image clearly shows, is no longer attached directly to the ice shelf, but has broken off and been displaced 1.7 km to the southwest.

The evidence for an ice cover on the S-shaped lead is the narrow, castellated, strong return running through the black area. The castellations strongly resemble finger-rafting, which occurs in young sea ice up to 0.30 m thick. The S-shaped lead, one of many in the pack ice at the time, the finger-rafting and the inferred ice thickness suggest that the calving occurred only a short time before the SAR overflight. Theoopening of leads in mid-winter in this region occurs during periods of persistent offshore geostrophic winds, which are the result of a high pressure cell over Greenland and a low pressure cell over the Canadian Arctic Archipelago (Ahlnäs and Sackinger, 1988). A weather pattern of this kind occurred from 12 February (Fig. 3b) to 15 February 1988 causing offshore winds with speeds of up to 10 m s^{-1}. This was only 7-10 days before the SAR data was acquired; hence, the calving of the Milne Re-entrant was detected in near-real-time.

In 1984 an MLSI floe of about 1½ km length and about 5 km width broke out of Yelverton Bay just west of the Milne Ice Shelf. Yelverton Bay remains a potential source of many such MLSI floes.

These thick floes are most hazardous to offshore structures in water depths as shallow as 10 meters. After one circuit of the Beaufort Gyre, however, thinning of these floes reduces their thickness to a value closer to the average multiyear pack ice thickness.

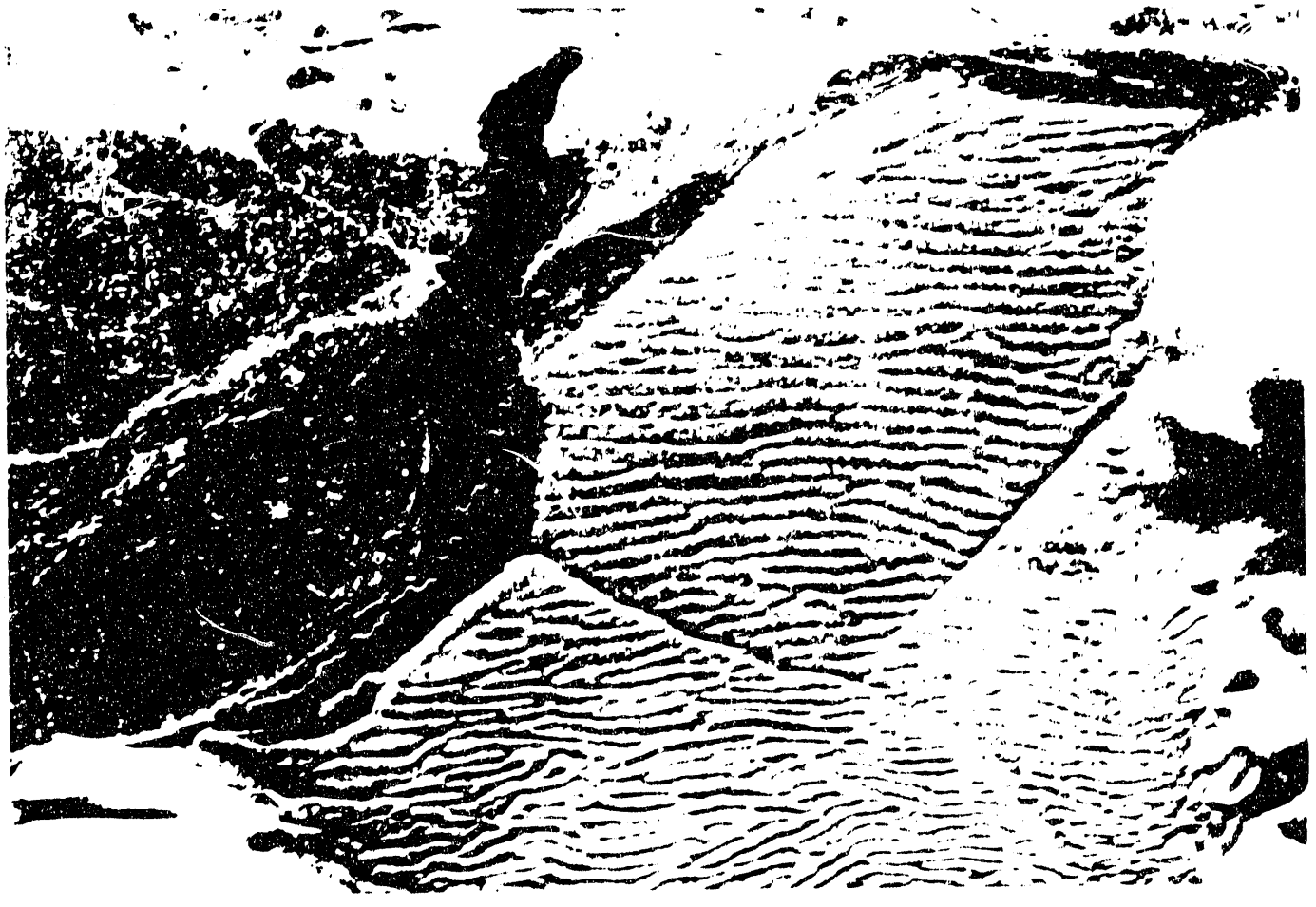

Figure. 3a: Airborne X-band synthetic aperture radar of the Milne Ice Shelf, 22 February 1988, showing the detachment of the Milne Re-entrant from the ice shelf. The dark, roughly S-shaped region is a refrozen lead separating the re-entrant and ice shelf.

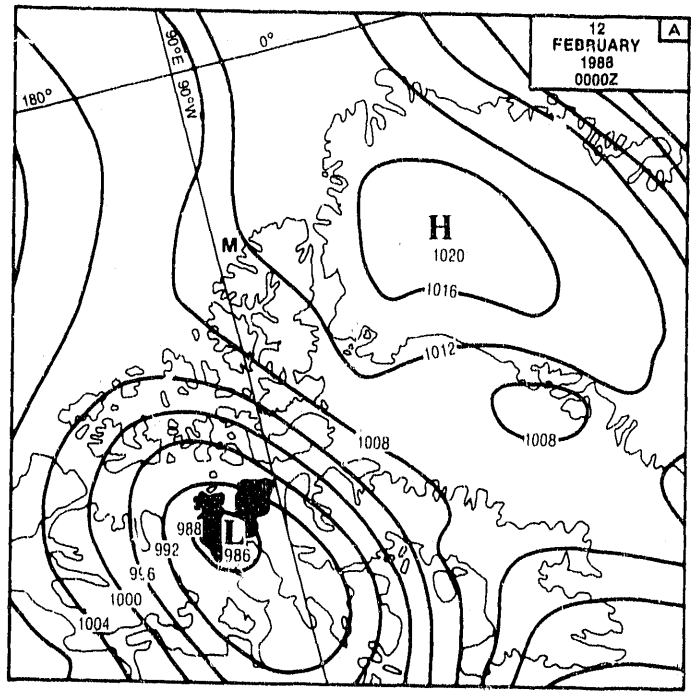

Figure. 3b: Pressure chart showing an anti-cyclonic system over Greenland and a cyclonic system over the Canadian Arctic Islands, which would have produced southerly or offshore winds across the north coast of Ellesmere Island and the Milne Ice Shelf (M) on 12 February 1988.

III. ICE ISLAND DRIFT AND DYNAMICS

As a consequence of aerial reconnaissance, the operationoof drifting research stations, and the deployment of satellite positioning systems and drift buoys on ice islands, much has been learned about the drift and dynamics of ice islands.

Long-term, large scale drift

Perhaps the best known ice island and the most familiar ice island drift path was that of T-3, the site of a drifting research station which operated almost continuously from 1952-1979. T-3 was first observed in July 1950 in the northern Chukchi Sea northwest of Point Barrow, but it was subsequently learned that it had been photographed from the air in April 1947 near Ellef Ringnes Island (Figure 4), (Koenig et al., 1952). Between 1947 and 1979 the ice island made at least three circuits of the Beaufort Gyre; two large diameter, outer circuits and, in the 1960s, one small diameter, inner circuit (Figure 4). In the early 1960s T-3 drifted parallel and close to the north coast of Alaska and for over 12 months in 1960-61 it became grounded near Pt. Barrow.

In late 1979, T-3 was abandoned and was not observed again until July 1984 in the vicinity of the southern tip of Greenland. The final <5 years of its drift were thus in the Transpolar Drift stream, an average movement trend which carries ice out of the Arctic Ocean through Fram Strait into the Greenland Sea. The drift track of ice island ARLIS-II exemplifies ice island motion in the Transpolar Drift stream (Figure 4). ARLIS-II was first observed in 1959 near Ellef Ringnes Island (Figure 4) but its drift was not recorded on a regular basis until May 1961, when a drifting research station was established on it, when it was located north of Pt. Barrow (Figure 4). ARLIS-II also took <5 years, from 1961 to 1964, to drift right across the Arctic Ocean. Unlike T-3, ARLIS-II never made a complete circuit of the Beaufort Gyre after its discovery. Both ice islands began the final years of their drift after crossing the 180^{o} meridian (Figure 4). The drift

paths of T-3 and ARLIS-II reflect the general motion of ice in the Arctic Ocean, which occurs in response to the large-scale, long-term atmospheric circulation.

Ice islands WH-5 and Hobson's Choice both calved from the East Ward Hunt Ice Shelf and they are the only ice islands to have had their drift monitored regularly after calving. Although they had the same source, their drift tracks were quite different from each other and from those of T-3 and ARLIS-II (Figure 4).

WH-5 was one of the five massive ice islands which calved from the Ward Hunt Ice Shelf in 1961-62 (Hattersley-Smith, 1963). Whereas four of the ice islands drifted westward, WH-5 drifted to the east and by February 1963, only 10 months after it had been discovered (April 1962), it had entered Nares Strait, the channel between Greenland and Eilesmere Island (Figure 4) (Nutt, 1966). The ice island disintegrated in July 1963, by October 1963 the fragments had entered northern Baffin Bay (Figure 4) and by May 1964 they were scattered from the northern tip of Labrador to the Grand Banks of Newfoundland (Nutt, 1966).

Hobson's Choice broke off the East Ward Hunt Ice Shelf in 1982-83 (Jeffries and Serson, 1983). By August 1988 it had drifted to a point just west of the northern tip of Ellef Ringnes Island, but then began to drift back towards the mouth of Peary Channel (Figure 4). By April 1990 Hobson's Choice, and evidently some of the other ice islands illustrated in Figure 1, were located in the channel, apparently within the fast ice rather than in drifting pack ice. Under the right circumstances, these ice islands could break out of Peary Channel and resume their drift in the Beaufort Gyre, or, they may continue to drift, albeit very slowly, through the inter-island channels of the Canadian Arctic Archipelago. This would not be without precedent; many ice islands were found in those channels in the late 1940s (Koenig et al., 1952).

The drift tracks shown in Figure 4 are just a small number of the infinite set of possible drift paths which ice islands may follow (Sackinger et al., 1990). Because of the need for a greater predictive capability regarding the occurrenceof ice islands in

waters where there exists a probability of an interaction with an offshore structure or vessel, a coupled Monte Carlo dynamic ice island drift model has been developed (Li, 1988). The computer simulation has appropriate, realistic treatments of, 1) driving forces, 2) ice island calving statistics, 3) ice island dimensions, including

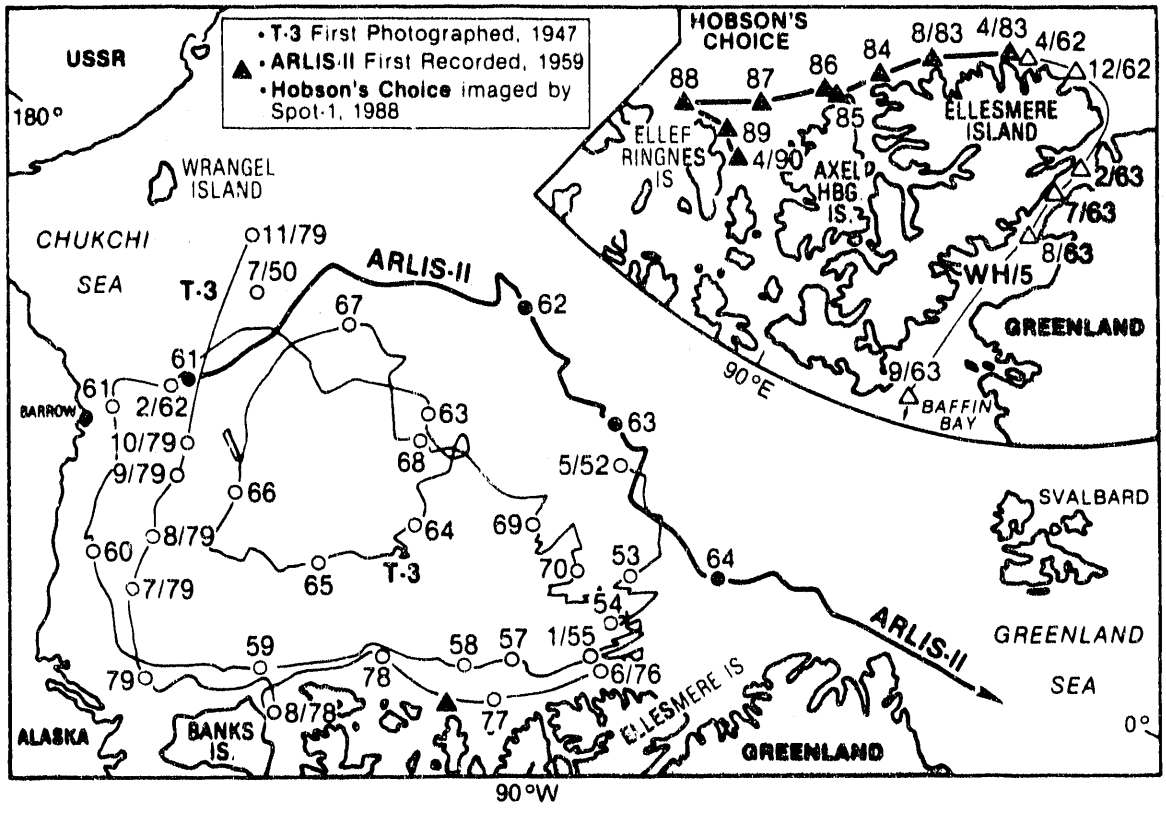

Figure. 4: Map of the drift tracks of ice islands T-3, ARLIS-II, WH-5 and Hobson's Choice in the Arctic Ocean and adjacent waters. For T-3 and ARLIS-II the dates are for January of a given year unless another month is identified. For Hobson's Choice the positions are for August of each year except April 1983. The T-3 and ARLIS-II data were made available by Dr. J. J. Kelley, Institute of Marine Sciences, University of Alaska Fairbanks. The WH-5 data are from Nutt[10]. The Hobson's Choice positions are from Argos satellite positioning buoys operated by the present authors.

thinning by ablation, and, 4) an Arctic Ocean simulation domain with possible exits through the land boundaries at the Bering Strait, Nares Strait and Fram Strait. One of many simulated ice island trajectories produced to date is shown in Figure 5. In this case, the simulated ice island originated from northernmost Ellesmere Island and subsequently drifted into the Greenland Sea via the Transpolar Drift, without completing a full circuit of the Beaufort Gyre. The ice island followed a somewhat tortuous route, particularly in the Beaufort Gyre adjacent to the Canadian Arctic Archipelago and in the central Arctic Ocean in the Transpolar Drift-Beaufort Gyre straddling the 180^{o} meridian (Figure 5).

One of the results of the Monte Carlo-dynamic ice island coupled model is that the recurrence interval for ice islands in coastal shelf regions of the Beaufort and Chukchi Seas is 10 to 100 years (Li, 1988). Offshore structure-ice island interaction thus has a sufficiently high probability that it must be considered.

Short-term, small-scale drift

The convoluted drift track simulated in Figure 5 is a series of irregular cycloidal motions and reversals. Similar motions have been observed in the drift of T-3 (Browne and Crary, 1958) and of Hobson's Choice (Lu, 1988). In the case of Hobson's Choice the irregular cycloidal motions and reversals occurred in response to changes in wind direction brought about by the alternation of anti-cyclonic and cyclonic systems over the Arctic Ocean (Lu, 1988). These motions have spatial and temporal scales of 10^{0} - 10^{2} km and days to weeks respectively.

A second type of elliptical motion not reproduced in Figure 5 occurs with a period of about 12 hours and a radius of about 0.5 km. These clockwise-only motions were observed when T-3 was located in the central Arctic Ocean in 1963 (Hunkins, 1967). Rather than being tidal motions they were considered to be inertial

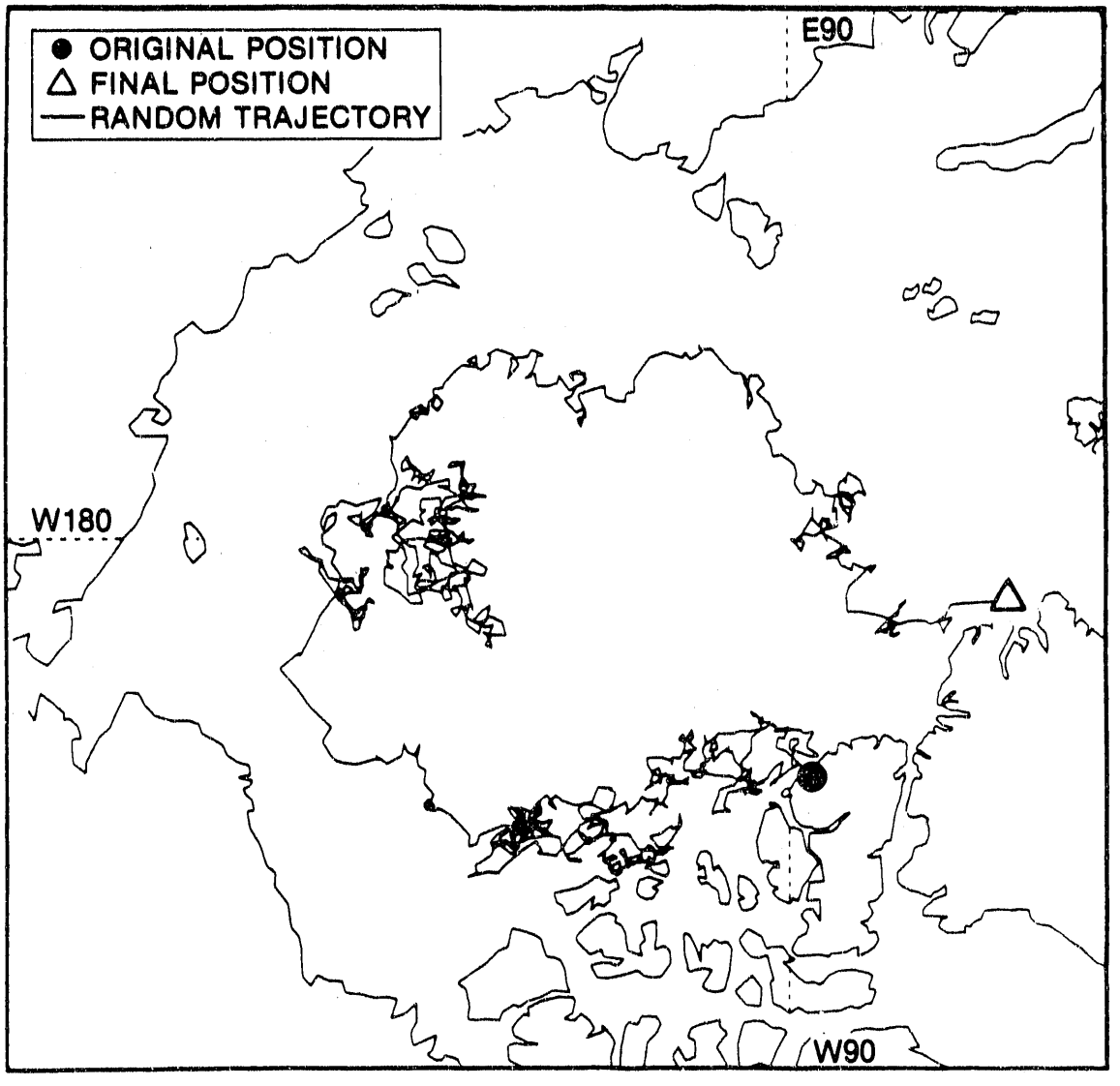

Fig. 5: Simulated drift trajectory for an ice island calving from the north coast of Ellesmere Island and exiting the Arctic Ocean via Fram Strait generated by a Monte Carlo-dynamic ice island drift model.

oscillations representing transient response of a floating ice mass to changing wind stress.

Even though the drift paths of T-3 and Hobson's Choice have been found to be highly convoluted at times, those two ice islands tended to maintain a near constant orientation or azimuth when they underwent motions and reversals (Browne and Crary, 1958; Hunkins, 1967; Lu et al., 1990). Ice islands appear to behave as classical rigid bodies in which translational and rotational motions are independent of each other (Hunkins, 1967). Based upon evidence from T-3, with a shelf ice length/width ratio of about 2, when rotations did occur they were always clockwise (Browne and Crary, 1958) and surrounding pack ice concentrations were reduced (Hunkins, 1967). More detailed analysis of rotations of Hobson's Choice (length/width ratio of 3.5) is in progress.

An example of small-scale motion of Hobson's Choice is illustrated in Figure 6, (Lu et al., 1990). During the two days, June 7-8, 1986, the wind speed remained in the range of 5 m/s to 7 m/s and generally from the same direction, 310^{o} to 325^{o}. The orientation of the long axis of the ice island varied only from $41^{o}41'48"$ on June 7 to $41^{o}44'14"$ on 8 June 1986. The lack of significant movement from 0000Z to 1200Z on June 7 is though to be due to currents, acting against the broadside of the ice island keel, opposing the wind stress. Pack ice stress against the ice island adds an additional force with unknown magnitude and direction throughout the 2-day movement episode. The motion in the time interval 1200Z to 2100Z on June 7, perpendicular to the direction of the wind is due to the orientation effect of the keel which still, however, provided sufficient form drag for the current effects to be displayed. Tidal currents and wind then reinforced each other for later times, motion was small, and the current effects were again balanced by wind shear on the ice island. Unfortunately, no water current velocity measurements were available during this episode to confirm these ideas.

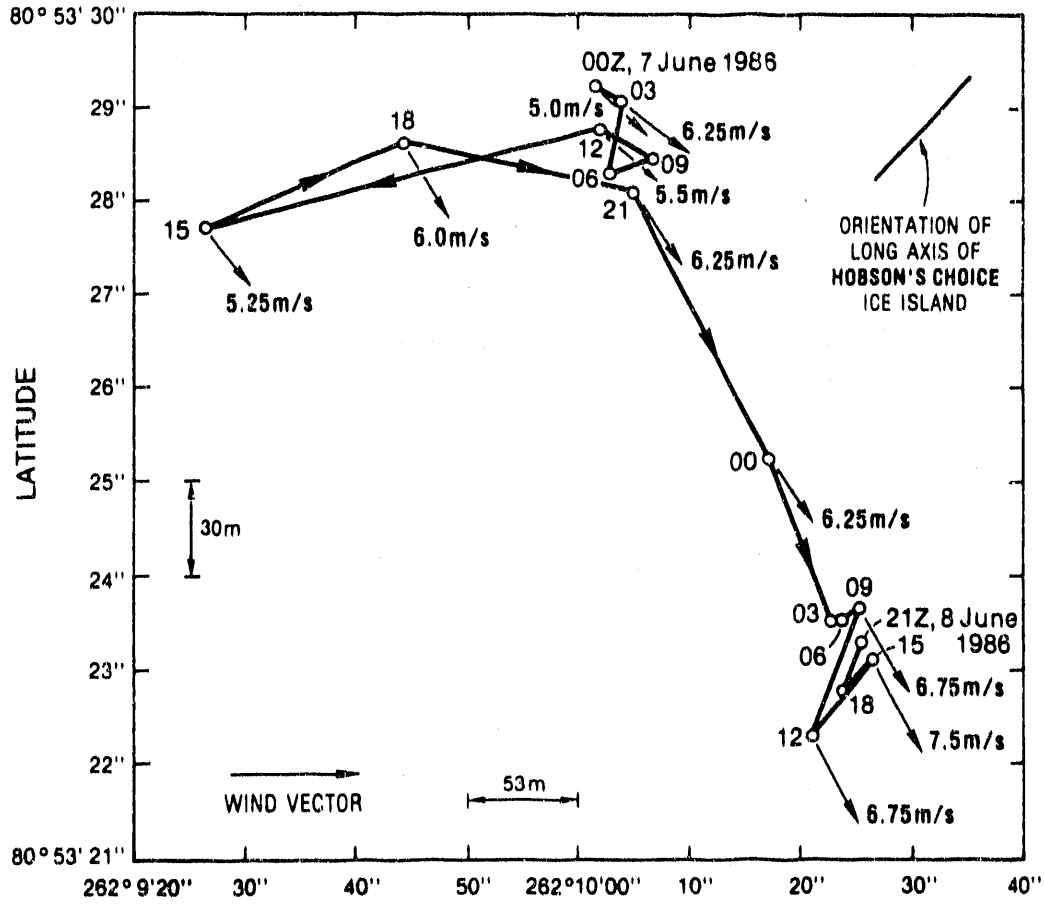

Fig. 6: Small-scale motion of Hobson's Choice, 0000Z 7 June 1986 t 2100Z 8 June 1986. The positions are from a satellite positioning system accurate to 30 m (Schmidt[16]); thus, the larger motions are real and not random instrument variations.

There are differences in motion between ice islands and sea ice at the smaller, shorter scales, as exemplified by their response to surface and geostrophic wind forcing. As discussed by Sackinger (1988), the ratio of sea ice speed to surface wind speed is 0.034 for smooth ice, and 0.025 for rough ice; the drift angle is 34^{o} for ice of 1 meter thickness and 25^{o} for iceoof 0.1 meter thickness. The ratio of sea ice speed to geostrophic wind speed is about 0.008, with the ice drifting about 8^{o} to the right of the wind (Thorndike and Colony, 1982). Recent analysis of the wind-driven motion of Hobson's Choice has shown that, on average, the ratiooof its speed to the surface wind speed is about 0.014 with a turning angle of 20^{o} to the right of the wind, while the ratio of its speed to the geostrophic wind speed is about 0.008 with a turning angle of 25^{o} to the left of the wind (Lu, 1988). Similar relations were obtained for T-3 (Browne and Crary[12]).

Several factors contribute to the variations in the response of ice islands and sea ice to the wind. Ice islands are deep draft features with greater mass and volume below the waterline as compared with sea ice; consequently, ice islands are subject to a considerable anisotropic water form drag which tends to reduce their speed for wind-driven events, while dominating their small-scale motion during current-driven events (Lu et al., 1990). On the other hand, because the Coriolis force per unit area acting on an ice island is greater than for an equal area of sea ice, the direction of the turning angles between an ice island and the surface and geostrophic winds may be expected to be greater than for sea ice. In the case of Hobson's Choice, a residual force, comprising primarily a pack ice force, counteracts the Coriolis force and reduces the turning angles. In some transient episodes, the pack ice force may even move the ice island to the left of the geostrophic wind. Ice island dynamics and the forces acting during movement events are discussed in some detail in Lu (1988) and Lu et al. (1990).

IV. ICE ISLAND PHYSICAL-STRUCTURAL-MECHANICAL PROPERTIES

As mentioned above, the largest ice island known today in the Arctic Ocean is the "Hobson's Choice" Ice Island which calved in 1982-83 from the East Ward Hunt Ice Shelf (Jeffries and Serson, 1983). The ice island comprises three ice components: 1) 16 km^2 of 42.5 m thick shelf ice; 2) 10 km^2 of 8-10 m thick multiyear landfast sea ice (MLSI) that was previously attached to the front of the ice shelf and which has remained attached to the shelf ice component since calving; 3) 7.75 km^2 of 5-6 m thick consolidated multiyear pack ice which has become attached to the ice island since the calving. The surface of the shelf ice component has a distinctive undulating topography (Figures 1 and 2a), similar to that of the Milne Ice Shelf (Fig. 3a). Since 1985, four ice cores have been obtained from the shelf ice component, three from hummocks and one from a depression. Here, we present some physical-structural-mechanical properties data for hummock core #86-1 and depression core #86-2 which were obtained 100 m apart (Jeffries et al., in press).

Both cores are 100% superimposed ice, a typeoof glacier ice formed by the thawing and refreezing of snowpack. Three sub-types have been identified; granular iced firn, (crystal diameters, 5-10 mm), columnar slush ice (crystal diameters, 10-20 mm) and columnar lake ice (crystal diameters, >20 mm). Ice core 86-1 comprises 75% iced-firn and 25% columnar ice. Ice core 86-2 comprises 60% iced-firn and 40% columnar ice. Each of the ice types has a very low liquid electrical conductivity. In core 86-1 conductivity values range from 2.3 to 252.0 mS cm^{-1} (mean 11.6 $\pm$ 32.8) and in core 86.2 the values range from 1.1 to 274.0 mS cm^{-1} (mean 6.3 $\pm$ 25.4). A value of 274.0 mS cm^{-1} is equivalent to a salinity of less than 0.2‰; thus, the ice has a very low level of dissolved impurities.

With colleagues at the National Research Council of Canada, Institute for Research in Construction, Geotechnical Section, we jointly conducted 25 closed-loop (constant strain rate uniaxial compressive strength tests (15 from core 86-1, 10 from

86-2) at numerous strain rates in the range of 2 X 10^{-7} to 1 X 10^{-3} s^{-1} and a temperature of -10°C (Jeffries et al., 1990). The results are presented as a stress-strain plot in Figure 7. Data from the initial Hobson's Choice mechanical property test program on surface specimens (Frederking et al., 1988), and data from some iceberg specimens from eastern Canada and Greenland (Sinha and Frederking, 1987; Lachance and Michel, 1988) are also presented in Figure 7.

The ice island strength values range from a minimum of 1.64 MPa at a strain rate of 2 X 10^{-7} s^{-1} to a maximum of 6.75 MPa at a strain rateoof 1 X 10^{-3} s^{-1}. Both these values are for specimens from core 86-1. Although the test program remains to be completed and more data acquired for individual specimens from each core, for a given strain rate specimens from core 86-1 appear to be slightly stronger than specimens from core 86-2. However, until the test program is completed and relationships between specimen strength and physical properties (bulk density, ice crystal size and structure) have been determined, it will not be possible to establish whether ice island hummock ice is stronger than depression ice.

On a more general level, the strength data from cores 86-1 and 86-2 compares closely with the initial ice island test data (Frederking et al., 1988) and with the iceberg ice tested by Sinha and Frederking (1987). On the other hand the ice island ice apparently is stronger than other iceberg ice specimens tested by Nadreau (1985), and Lachance and Michel (1985). This may be due to physical property differences, particularly differences related to iceberg ice generally forming more slowly at high elevations on glaciers/ice sheets where the effects of meltwater in snowpack are minimal compared to the shelf ice formed at sea level.

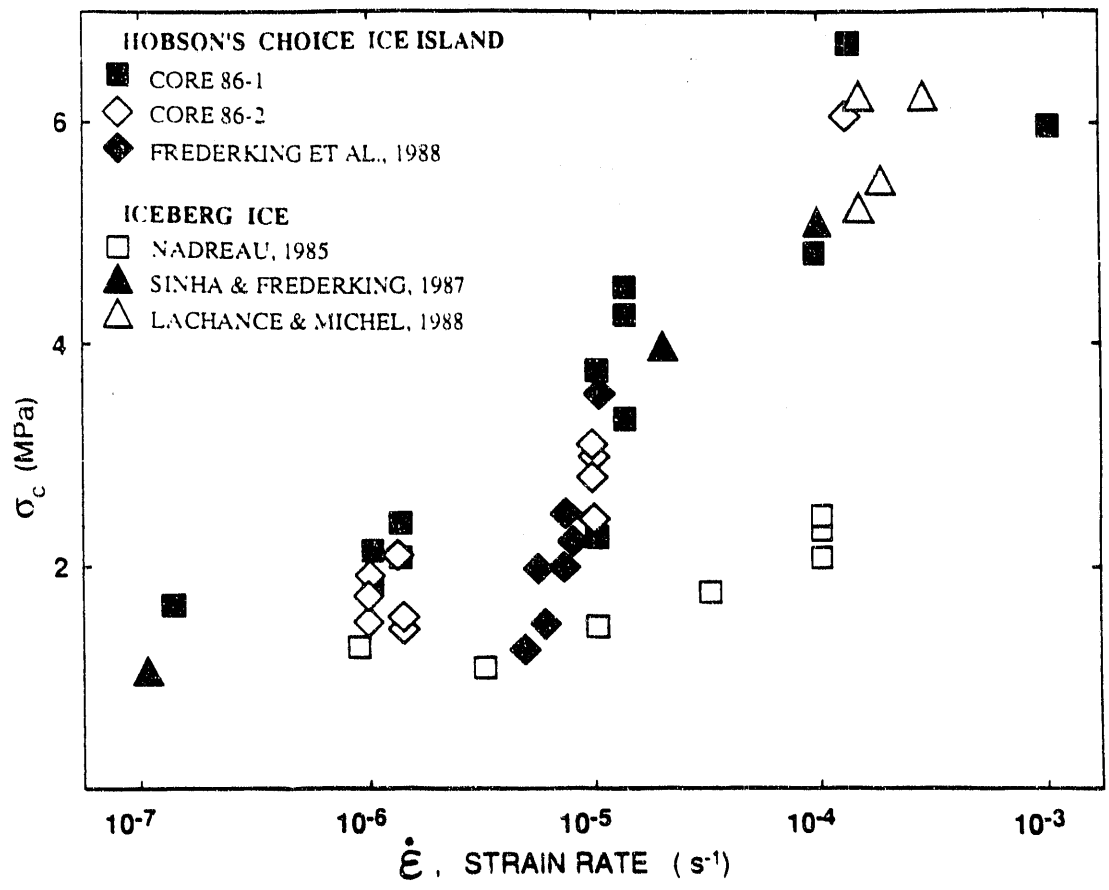

Fig. 7: Uniaxial compressive strength (s_C) as a function of strain rate for ice specimens from Hobson's Choice Ice Island, and from icebergs.

V. ICE ISLAND-STRUCTURE INTERACTIONS

Approach of ice islands toward structures

During conditions of wind speed greater than 5.25 m/sec., the wind is a dominant driving force for ice islands in deep (<400m) water (Lu et al., 1990). In shallow water, (<75 meters), the water velocity is increased in the narrow gap (h) between the bottom of the ice island and the sea floor. Water drag will increase, and the relationship between wind speed and ice island speed would definitely be reduced, since, to the first approximation, the relative water velocity under the ice island increases inversely linearly with the spacing, h, and the water drag increases with the square of the relative water velocity. As the water velocity above the sediments increases for small h, sediment suspension, liquefaction and lateral transport may be expected. The density of the sediment-laden water is greater, as well, leading to an increase in water drag. An increase in the water height difference between the front and trailing boundaries of the ice island would also occur, helping to decelerate the ice island.

Persistent currents, which are channeled into the narrow spacing, h, between the ice island and the sea floor, would tend to dominate the force balance relation and steer an ice island in the average direction of the current. Deliberate grounding or near-grounding of an ice island on a submerged seafloor barrier would appear to be worthy of consideration as a passive defense for a nearby offshore structure.

An ice island is likely to be surrounded by a zone of multiyear ice (MYPI) which has formed around it during its drift (see Section II). As this ice surrounds the old shelf ice, except at the ends, there is a very high probability that the type and thickness of ice which fractures against a structure will be the MYPI as described above. Ice fracture will therefore take place in a relatively weak, thin ice zone. In response to tidal current forcing , and as a consequence of the increased draft of the ice island shelf ice component, there is very often a region of cracking at the outer boundary of the MYPI.

This region contains thin, recently-refrozen ice and rubble fragments. It provides several hundred meters of a thin-ice buffer zone for energy absorption before the actual thick ice island is in direct contact with the structure. Whether this is sufficient to bring the ice island to a halt must be determined by further analysis.

To the above discussion of energy loss factors during grounding must be added the damping resulting from the hydrodynamic response (Luk, 1983). For a water depth of twice the thickness of the ice island, an added mass coefficient of 0.4 for surge motion, and larger values for heave and pitch motion, are possible (Luk, 1983). Damping coefficients are a function of interaction geometry and of frequency, expressing the energy loss involved in the generation of surface and internal outgoing water waves. These should be evaluated for particular expected situations. The increase in the turbid water effective density due to the suspended sediments represents a modification to be incorporated into the early pioneering theory of Luk (1983).

Progressive contact with structures

As an ice island/MLSI/MYPI composite mass approaches a grounded offshore structure, the assumption may be made that the water depth is greater than the depth of the thick shelf ice keel of the composite. For example, Hobson's Choice ice island has an original shelf ice thickness of about 42 meters and a keel extending a nominal 38 meters below the waterline. An offshore oil development structure in the Chukchi Sea may be built in a water depth of 45 meters, for example. The shelf ice keel depth will be reduced each year as the ice island thickness is reduced during its drift.

In water depths of 25 meters or less, one design concept includes a sloping structure surface to cause flexural failure of sea ice, and a smaller total lateral load. A recent treatment by Sanderson (1988) described several details of interactions between sea ice and structures. The cracks in the ice were shown, in research by

Sanderson and his collaborators, to be important in the initiation of fractures in sea ice in contact with structures. The naturally-occurring cracks in the ice island/MLSI/MYPI composite mass remain an uninvestigated subject today, although thermal cracks in the top surface of ice island T-3 were reported to be up to 1 cm wide with 15 m average spacing (Holdsworth and Traetteberg, 1974). Vertical-walled structures, such as the CIDS and SSDC (Sanderson, 1988), have been proven in winter moving ice conditions and, because of their lower cost, similar designs will probably be chosen for offshore production platforms. The progressive contact of the MYPI and MLSI portions of the composite ice islands with a vertical-walled structure will first produce a zone of rubble ice via a mixed-mode failure. Energy is absorbed by ice fracture, by up-thrusting and down-thrusting of ice rubble, by small motions (e.g. damped variations) in the structure foundation sediments, and by the excitation of traveling hydrodynamic waves and acoustic waves in the water and in the ocean floor. Ice rubble, once formed, may ground on the seafloor if the water depth near the structure is less than about 25 meters, and in such a case, the grounded rubble will form an additional barrier to resist the forward motion of the composite ice island. Energy is absorbed more effectively by such grounded rubble, as more water wave excitation takes place, and some energy is dissipated in the sea floor under the grounded ridge. If rubble, once formed, simply clears around the structure, this advantage is lost. In water deeper than 25 meters, this would be quite probable. The MLSI and MYPI failure models against a vertical-walled structure have not been studied.

If the end of the shelf ice section of the composite ice island strikes the structure (a less likely event because of its smaller cross-section), a zone of small ice fragments ("ice-powder") may be expected initially at the contact area. This zone progressively grows in area and in extent, and part of the "ice-powder" will be extruded out of the free surfaces at the top and bottom of the contact space. Stresses will be transmitted

through the "ice-powder" to the fracture surface boundary, which will grow until the composite ice island comes to rest or until the offshore structure starts to slide across the seafloor. In each particular circumstance, the attachment of the structure to the sea bed should be firm enough to resist sliding motion up to a "breakaway point," and then, prior to the onset of structure damage, the structure may be allowed to go into a planned, deliberate sliding mode. Wellhead integrity would be assured by sub-seafloor failsafe blowout prevention equipment which, presumably, could be re-entered later without heroic measures. Studies of the progressive interactions and growth of the ice rubble and "ice-powder" failure zones remain to be undertaken. The formation of ice rubble against a structure, for the composite ice island moving broadside against the structure at expected speeds, may permit the floe to come to rest before the thick shelf-ice core actually touches the structure; this needs to be verified.

Possible countermeasures in ice island/structure interaction

One strategy for ice island defense is to break the thick shelf-ice core into fragments, by using seawater pumped into the elongated lakes in the summer (thus introducing brine on top of the low-salinity shelf ice). A second technique is to add artificial spray sea ice to edge locations in winter, causing abnormal gravity loading and possible flexural failure locally. Explosives have been tried with limited success (Mellor et al., 1977).

Construction of seafloor obstacles near an offshore structure, perhaps in the form of large precast caissons or steel barges that can be ballasted, or even attached with pilings into the seabed, is another option. Ice rubble would form on such underwater obstacles, as the annual ice ridge keels pass over the obstacles. Grounding of ice ridge keels on natural shoals in the Chukchi Sea is a well-known effect (Barrett and Stringer, 1978). There is commonly an open-water region near

such shoals. Planning for optimum placement of such underwater barriers on a site-specific basis remains for the future.

The retention of ice rubble near a structure, and the artificial thickening and grounding of ice rubble by using spray sea ice, also should be considered. This type of barrier, while effective in winter, would have to be made to a thickness of 30 meters or more in order to survive through most or all of the summer. A permanent grounded ice feature, made of artificial spray sea ice and replenished each winter, may be possible in certain offshore locations.

The deliberate addition of artificial sea ice by seawater flooding on top of a grounded ice island has been done (Sanderson, 1988), and the use of spray sea ice to thicken ice islands is possible as well. For a floating ice island moving towards a region in which offshore structures are located, one defense countermeasures option to consider is the addition of spray ice to increase the keel depth so that grounding takes place in water deeper than that found at the offshore structure location.

Many other options for defense against ice islands will undoubtedly be proposed. The tracking of ice island locations using satellite-positioning buoys and imaging systems is important for the ice islands that are known to be drifting in the Arctic Ocean, so that probabilities of their interaction in chosen oil-development locations can readily be established. A real-time warning of a threatening ice island can also thus be available.

VI. CONCLUSIONS

Drifting ice islands and thick undeformed sea ice floes are formed in the coastal regions of Ellesmere Island, and in other arctic high latitude bays and fiords. They range in thickness from 6 meters to 60 meters, have lateral dimensions of up to 29 km, and length-to-width ratios from 1 to 6. They are often surrounded by and attached to

multiyear landfast sea ice (MLSI) and by multiyear pack ice (MYPI), forming a composite floe with shelf ice at the center.

Paths of ice islands differ from those of the surrounding sea ice because of the greater keel depth and because of the larger mass per unit area. Differential motion leads to pack ice stresses and ice rubble formation on the ice island boundary, which builds into MYPI by summer melting and refreezing processes. Ice island drift paths contain many fine details of wind-driven and current-driven motions superimposed on their large-scale circulation around the Arctic Basin.

Interactions with structures first involve an increase in water drag forces in shallow water, followed by a sequence of ice rubble fragments created as the MYPI and MLSI interact with the structure and any pre-existing ice rubble piles.

Countermeasures are suggested, including ice island fragmentation, sea floor obstacles, and ice island/spray ice modifications. Additional research on ice island/structure interactions is recommended.

VII REFERENCES

Ahlnäs, K. and W. M. Sackinger, 1988. Offshore winds and pack ice movement episodes off Ellesmere Island. In, Port and Ocean Engineering under Arctic Conditions, Vol. III, W. M. Sackinger and M. O. Jeffries (Eds.), Geophysical Institute, University of Alaska Fairbanks, 271-286.

Barrett, S. A. and W. J. Stringer, 1978. Growth mechanisms of 'Katie's Floeberg,' Arctic and Alpine Research 10, pp. 775-783.

Browne, I. M. and A. P. Crary, 1958. The movement of ice in the Arctic Ocean, in Arctic Sea Ice, Proceedings of the Conference held at Easton, Maryland, February 1958. National Academy of Sciences--National Research Council Publication 598, 191-209.

Frederking, R. M. W., G. W. Timco, M. O. Jeffries, and W. M. Sackinger. Initial measurements of physical and mechanical properties of ice from Hobson's Ice Island. Proceedings of the 9th International Symposium on Ice, IAHR, Vol. 1, 23-27 August 1988, 188-198.

Holdsworth, G. and A. Traetteberg, 1974. Deformation of an arctic ice island, Proceedings of the 2nd International Conference on Port and Ocean Engineering under Arctic Conditions, Iceland, 419-440.

Hunkins, K., 1967. Inertial oscillations of Fletcher's Ice Island (T-3), *J. of Geophys. Res. 72 (4)*:1165-1174.

Jeffries, M. O., 1987. The growth, structure and disintegration of arctic ice shelves: a review, Polar Record 23 (147):631-649.

Jeffries, M. O. and H. Serson, 1983. Recent changes at the front of the Ward Hunt Ice Shelf, Ellesmere Island, NWT, Arctic 36:289-290.

Jeffries, M. O. and W. M. Sackinger, 1989. Analysis of interpretation of an airborne synthetic aperture radar image of Hobson's Choice Ice Island, 10th International Symposium on Port and Ocean Engineering under Arctic Conditions, Luleå, Sweden, 12-16 June, 1989, Volume 2, 1032-1041.

Jeffries, M. O., W. M. Sackinger and H. D. Shoemaker, 1988. Geometry and physical properties of ice islands, In, Port and Ocean Engineering under Arctic Conditions, Vol. 1, W. M. Sackinger and M. O. Jeffries (Eds.), Geophysical Institute, University of Alaska Fairbanks, 69-83.

Jeffries, M. O. and W. M. Sackinger, 1990. Near-real-time airborne synthetic aperture radar detection of a thick sea ice floe calving at the Milne Ice Shelf, and the contribution of offshore winds, in Ice Technology for Polar Operations, T. K. S. Murthy, J. G. Paren, W. M. Sackinger, and P. Wadhams (eds.), Computational Mechanics Publications, Southhampton, 321-331.

Jeffries, M. O., H. V. Serson, H. R. Krouse and W. M. Sackinger, In press. Ice physical properties, structural characteristics and stratigraphy in Hobson's Choice Ice Island and implications for the growth history of the East Ward Hunt Ice Shelf, Canadian High Arctic. *J. of Glaciology.*

Jeffries, M. O., N. K. Sinha and W. M. Sackinger, 1990. Failure stress and failure modulus of natural ice island ice under uniaxial compression of constant strain rates. Proceedings of the 9th International Conference on Offshore Mechanics and Arctic Engineering, Vol. 4, 18-23 February 1990, Houston, Texas, 223-229.

Koenig, L. S., K. R. Greenaway, M. Dunbar and G. Hattersley-Smith, 1952. Arctic Ice Islands, Arctic 5:67-103.

Lachance, J. and B. Michel, 1988. Experimental study of the brittle behaviour of iceberg ice. In, Port and Ocean Engineering under Arctic Conditions, Vol. III, W. M. Sackinger and M. O. Jeffries (Eds.) Geophysical Institute, University of Alaska Fairbanks, 11-19.

Lu, Ming-chi, 1988. Analysis of ice island movement, M. S. Thesis, University of Alaska Fairbanks, Fairbanks, Alaska.

Lu, Ming-chi, W. M. Sackinger and F.-C. Li., 1990. Analysis of ice island dynamics, Second International Conference on Ice Technology (ICT '90), 18-20 September, Cambridge, England, 241-256.

Luk, C.-H., 1983. Added mass and damping for ice floes by long water wave theory, Proceedings of the Offshore Technology Conference, Houston (OTC 4458), 133-142.

Mellor, M., A. Kovacs and J. Hnatiuk, 1977. Destruction of ice islands by explosives, Proceedings of the Fourth International Conference on Port and Ocean Engineering Under Arctic Conditions (POAC-77), St. Johns, Newfoundland, pp. 753-765.

Nadreau, J. P., 1985, Lois de comportement et de fluage de la glace granulaire simules de cretes de pression, Ph.D. Thesis, Civil Engineering Department, Laval University, Quebec.

Nutt, D. C., 1966. The drift of ice island WH-5, Arctic 19:244-262.

Sackinger, W. M., 1988. Coastal ice dynamics, In Arctic Coastal Processes and Slope Protection Design, A. T. Chen and C. B. Leidersdorf (Eds.), American Society of Civil Engineers, New York, pp. 63-84.

Sackinger, W. M., M. O. Jeffries, F.-C. Li and M.-C. Lu, 1990. Interaction of arctic offshore structures with drifting ice islands and thick sea ice floes, in Ice Technology for Polar Operations, T. K. S. Murthy, J. G. Paren, W. M. Sackinger, and P. Wadhams (eds.), Computational Mechanics Publications, Southampton, 211-228.

Sanderson, T. J. O., 1988. Ice Mechanics--Risks to Offshore Structures, Graham and Trotman, London, 253 pp.

Schmidt, M., 1986. Ice island navigation data, Geological Survey of Canada, Geophysical Surveys, Hazards and Terrain Sciences Branch, Geodynamics Section, Report 1986.

Shreider, Yu. A., 1962. The Monte Carlo Method, Pergamon Press.

Sinha, N. K. and R. Frederking, 1987. Preliminary observations on compressive strength, deformation and Poisson's ratio of iceberg ice. National Research Council of Canada, Technical Memorandum 141 (NRCC 28003), 413-429.

Spedding, L. G., 1977. Ice island count, southern Beaufort Sea, 1976, Report IPRT-13ME-77, APOA Project 99-3, Arctic Petroleum Operators Association, Calgary, Alberta, Canada, 50 pp.

Thorndike, A. S. and R. Colony, 1982. Sea ice motion in response to geostrophic winds, *J. Geophys. Res. 87* (C8):5845-4852.

Walker, E. R. and P. Wadhams, 1979. Thick sea ice floes, Arctic 32:140-147.

DATE
FILMED
01/08/93